

A TOF-E detector for ERNA recoil separator

M. De Cesare¹, A. Di Leva³, D. Schürmann³, L. Gialanella², F. Strieder³,
R. Kunz³, D. Rogalla³, N. De Cesare⁴, A. D'Onofrio¹, G. Imbriani², C. Lubritto¹,
A. Ordine², A. Palmieri⁴, V. Roca², C. Rolfs³, M. Romano², F. Schümann³,
F. Terrasi¹, and H.P. Trautvetter³

¹ Dipartimento di Scienze Ambientali, Seconda Università di Napoli, Caserta and INFN, Napoli, Italy

² Dipartimento di Scienze Fisiche, Università Federico II, Napoli and INFN, Napoli, Italy

³ Institut für Physik mit Ionenstrahlen, Ruhr-Universität Bochum, Bochum, Germany

⁴ Dipartimento di Scienze della Vita, Seconda Università di Napoli, Caserta and INFN, Napoli, Italy

⁵ Dipartimento di Scienze Ambientali, Seconda Università di Napoli, Caserta, Italy

Abstract. For improved cross-section measurements of the reaction ${}^4\text{He}({}^3\text{He},\gamma){}^7\text{Be}$ in inverse kinematics, the recoil mass separator ERNA (European Recoil separator for Nuclear Astrophysics) is used to detect directly the ${}^7\text{Be}$ recoils with high efficiency. The ${}^7\text{Be}$ recoils are produced by the ${}^4\text{He}$ projectiles in a windowless ${}^3\text{He}$ gas target. ERNA fulfils the requirement to study the reaction over the center of mass energy range $E_{cm} = 0.7\text{-}3$ MeV. In the energy range $E_{cm} = 1.1\text{-}3$ MeV ions identification is performed with $\Delta E\text{-}E_{Rest}$ telescope detector, while in the energy range $E_{cm} = 0.7\text{-}1.1$ MeV a TOF-E detector is needed. The commissioning of the TOF-E (Time of Flight-Energy) detector set up and the first observation of the ${}^7\text{Be}$ recoils are reported.

Key words. Recoil Separator - TOF-E detector

1. Introduction

The reaction ${}^4\text{He}({}^3\text{He},\gamma){}^7\text{Be}$ ($Q=1.586$ MeV) takes place in the Big Bang nucleosynthesis and in the pp-chain (Rolfs & Rodney 1988; Haxton 1995; Serpico et al. 2004).

The ${}^4\text{He}({}^3\text{He},\gamma){}^7\text{Be}$ reaction in the Big Bang nucleosynthesis is important to determine the abundance of ${}^7\text{Li}$, which is produced by electron capture of ${}^7\text{Be}$. Interest stems from the fact that there is less ${}^7\text{Li}$ observed in the universe than expected.

Send offprint requests to: L. Gialanella

In the pp-chain the determination of the ${}^4\text{He}({}^3\text{He},\gamma){}^7\text{Be}$ cross section is important for high energy solar neutrino flux determination (i.e. flux of ${}^8\text{B}$).

So far, two experimental methods have been adopted to measure the reaction cross-section. The first method is based on the collection of the ${}^7\text{Be}$ nuclei produced and the determination of their amount by means of the detection of the gamma-rays following the ${}^7\text{Be}$ decay to the first excited state in ${}^7\text{Li}$.

The second method is based on the detection of γ -rays from the ${}^4\text{He}({}^3\text{He},\gamma){}^7\text{Be}$ reac-

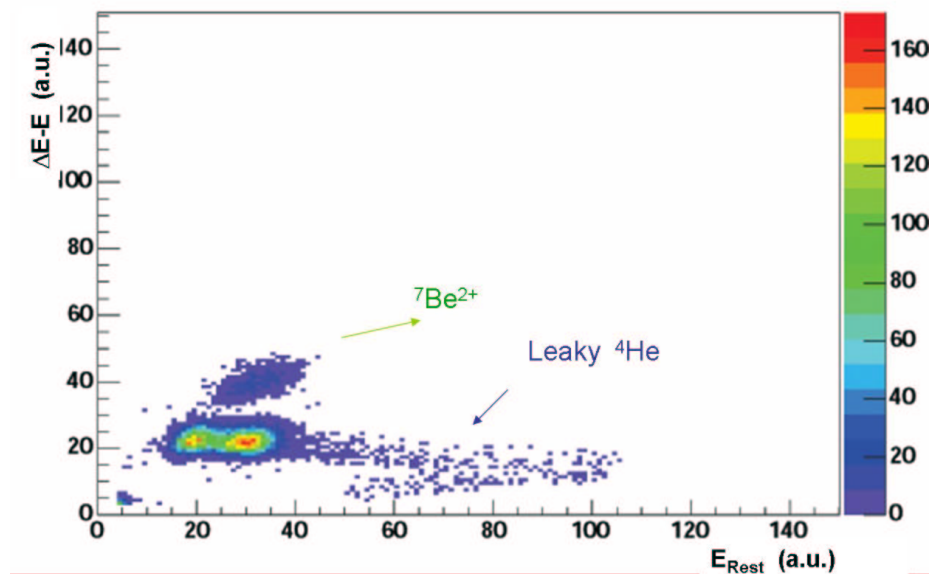


Fig. 1. The matrix shows ΔE again E_{Rest} of the ions, in arbitrary units. It is possible to see the spot of ${}^7\text{Be}^{2+}$ recoils and the ${}^4\text{He}$ leaky beam. This is a ${}^4\text{He}^{2+}$ beam at $E_{{}^4\text{He}^{2+}} = 3$ MeV ($E_{cm} = 1.3$ MeV).

tion. The discrepancy between these two methods is larger than 2σ (Adelberger et al. 1998), even if one introduces the results of the two last reaction cross-section measurements (Singh et al. 2004; Bemmerer et al. 2006), whereas no inconsistency is found in a separate analysis of each of the two groups of experiments. That suggests systematic error in at least one of the two methods, or a possible non-radiative contribution (Adelberger et al. 1998). To improve the situation, a new experimental approach has been undertaken at the 4 MV Dynamitron tandem accelerator in Bochum, called ERNA (Rogalla et al. 1999, 2003; Gialanella et al. 2004; Schürmann et al. 2004). In this approach, the reaction is initiated in inverse kinematics. The ${}^4\text{He}$ ion beam is guided into a windowless ${}^3\text{He}$ gas target and the ${}^7\text{Be}$ recoils emerge from the target together with the projectile beam. Immediately after the gas target the ratio between the number of recoils and ion beam particles is about 10^{-14} . After the gas target the separator suppresses the ${}^4\text{He}$ beam by means of velocity and rigidity filters, while the recoils, in a selected charge state, are transported to the

final detector. After the separator the ratio between the number of recoils and leaky beam particles (the beam that pass through the separator) is of the order of 10^{-2} . At the end of the separator there is the detection system where the ions are detected and identified. The possibility of ion identification is a crucial point, since it allows to suppress the portion of the incident beam that leaks through the separator. Additionally, it is possible to perform coincidence measurements between the prompt γ -rays and the recoils using a NaI detector array located at the target position.

ERNA fulfils the requirements to study the reaction over the center of mass energy range $E_{cm} = 0.7$ -3 MeV. In the energy range $E_{cm} = 1.1$ -3 MeV measurements can be performed with a ΔE - E_{Rest} telescope detector (Rogalla et al. 1999; Di Leva 2002). Fig. 1 shows a ΔE - E_{Rest} matrix at $E_{cm} = 1.3$ MeV. It is clearly possible to see that the separation between the ${}^7\text{Be}$ recoils and the ${}^4\text{He}$ leaky is small and diminishes at lower energy. For $E_{cm} < 1.1$ MeV ions identification becomes impossible and a different detector with lower detection energy threshold

is needed, i.e. a TOF-E detector. In this contribution the commissioning of such a TOF-E detector set up and the first observation of the ^7Be recoils at selected energies are reported.

2. TOF-E detector set up

Generally, a TOF-E system has a start and a stop detector and another one to measure the ion energy. In our set up, shown in Fig. 2, the start signal is given by a MCP (Microchannel Plate - Wiza 1979) mounted in electrostatic mirror configuration (Busch et al. 1980; Starzecki et al. 1982; Kuznetsov et al. 2000), the energy is measured by a 16 strips silicon detector, which also provides the stop signal (Di Leva 2002; De Cesare 2006).

Briefly, ions pass through a thin carbon foil ($4\text{-}26 \mu\text{g}/\text{cm}^2$ with a diameter of 45 mm) placed orthogonal to the beam axis and they are detected by a silicon detector. Electrons are stripped from the carbon foil due to the interaction of the impinging ions with the carbon foil. They are accelerated to at least 1 keV in the electric field generated by an acceleration grid (wires have a diameter of $25 \mu\text{m}$ and they are distant 1 mm from each other; 97.5 % transparency) that is parallel to the carbon foil. Since most of the electrons are stripped from the carbon foil with an energy of a few eV, after acceleration, they have approximately the same energy and their velocity direction is almost parallel to the beam axis. The distance between the acceleration grid and the carbon foil is 3 mm.

An additional grid is mounted in front of the carbon foil, but in opposite position of the acceleration grid and is kept at the same potential as the acceleration grid to prevent carbon foil deformation and/or breakage due to the electrostatic force. The electrons are bent, by means of an electrostatic mirror, towards the MCP, that has a diameter of $\phi = 40 \text{ mm}$, placed outside of the beam axis. The mirror consists of two parallel grids (internal and external grid, 5 mm distance) placed at 45° to the beam axis. The electrostatic field between these two grids bends the electrons through 90° towards the MCP. Since the acceleration grid, the internal grid and frame of the MCP are all at same po-

tential, electrons in the space between do not experience any force and they proceed along straight lines.

The trajectories of two electrons emitted from two different points of the carbon foil are shown in Fig. 3. The parabola branch in the space between the two grids of the electrostatic mirror is the same for all electrons. That means, as it is possible to obtain by simple geometrical consideration, that all electrons cover the same distance independently from the point where they are emitted. The isochronism of the trajectory is a fundamental requirement to obtain a good time resolution of the TOF-E system.

Fig. 2 also shows a configuration for picking up the signal that comes from the MCP based on a conic anode capacitively connected to the flat anode of the MCP assembly. This configuration allows a proper matching to the cable impedance and hence to avoid reflections that may influence the time resolution.

If the distance between start and stop detectors (L) is known, measuring Δt_{TOF} between start and stop, (that is equal to L/v , v is the velocity of the ion) and knowing the relation between the velocity and the kinetic energy (E) of the ion, one obtains:

$$\Delta t_{TOF} = L \cdot \left(\frac{m}{2E} \right)^{1/2}$$

where m is the mass in the non relativistic approximation: $v \ll c$.

This means that if Δt_{TOF} as a function of the energy of the ions is plotted, it is possible to distinguish ions with different mass because they will arrange on different curve.

3. Results

In 2006 the TOF-E system detector has been installed at ERNA for commissioning (Di Leva 2002; De Cesare 2006). Below are shown the results that we obtained with this set up.

3.1. Time resolution of the TOF-E system

The time resolution of the TOF-E detector (between the MCP and the silicon detector) is 0.7

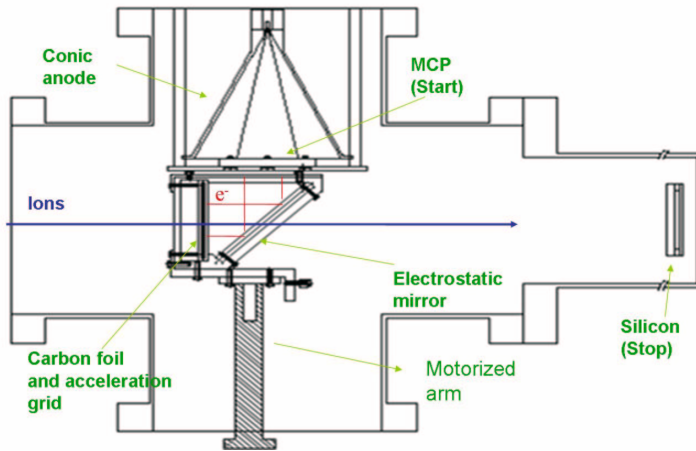


Fig. 2. TOF-E detector set up.

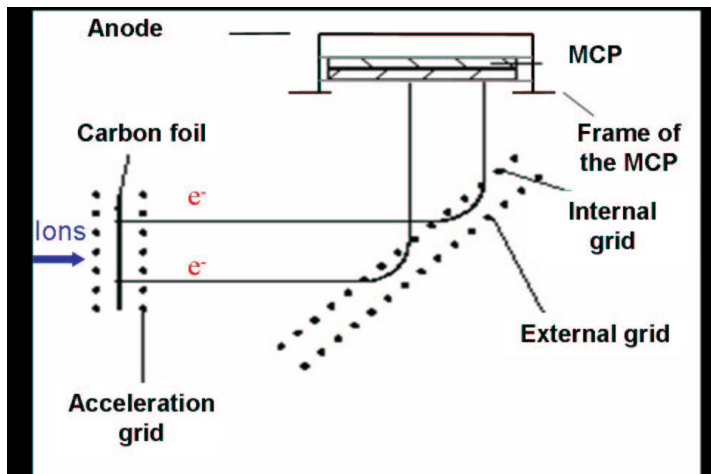


Fig. 3. MCP mounted in electrostatic mirror configuration.

ns. This is the result obtained with a $^{12}\text{C}^{2+}$ beam at $E_{^{12}\text{C}^{2+}} = 7$ MeV. For preventing a TOF-E detector breakage due to the high rate of the ions, the beam intensity was reduced to have a counting rate of about 300 Hz.

3.2. Position dependent efficiency

A low enough detection and ion identification energy threshold, a high and well known detection efficiency and also, a position indepen-

dent efficiency are key requirements for the TOF-E detector.

Since the recoils reach the position where the carbon foil is located distributed in a circle of 20 mm from the beam axis, it is necessary to verify the independence of the detection efficiency over such area. A beam of $^7\text{Li}^{1+}$ at $E_{^7\text{Li}^{1+}} = 1.0$ MeV was used. Also in this case for preventing a TOF-E detector breakage due to the high rate of the ions, the beam intensity was kept low enough to have a counting rate below 300 Hz.

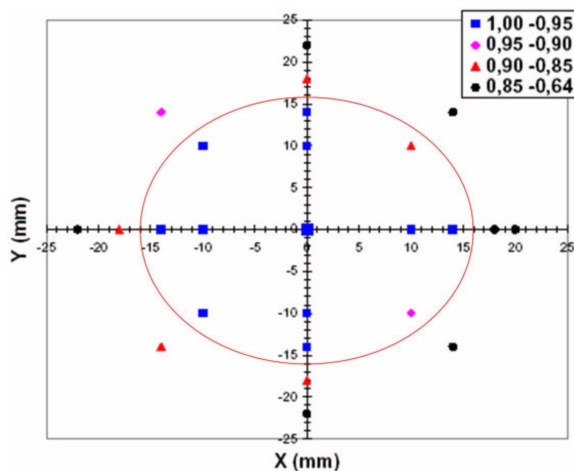


Fig. 4. Position scan efficiency along the carbon foil without the lens (De Cesare 2006). In the legend the different geometrical forms with different colors are for the different range of efficiency.

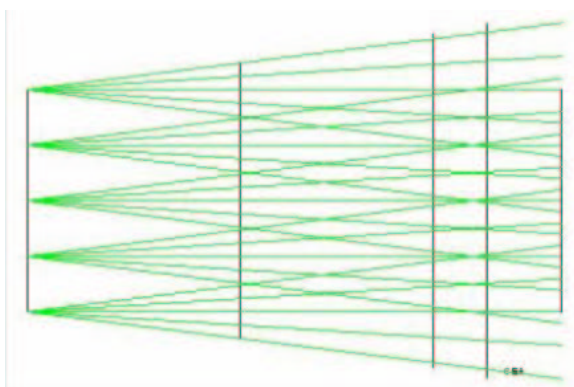


Fig. 5. From the left to the right respectively the carbon foil, electrostatic mirror, electrostatic mirror support, MCP support and the MCP. We can see that not all the electrons (green line) reach the MCP. The calculation is performed with COSY infinity.

The beam spot on the carbon foil, a square of $2 \times 2 \text{ mm}^2$, was defined by means of a slit system located directly in front of it.

The surface scan in Fig. 4 shows that $\sim 100\%$ efficiency is reached only within 15 mm to the geometrical axis. This loss may be explained by a non proper transport of the electrons to the MCP, as shown in Fig. 5, where the results of a Cosy Infinity (Makino & Berz 2002) calculation of the electron trajectories are reported.

To improve this situation a lens for focusing the electrons within the MCP will be in-

stalled. The influence of this lens on the electron trajectories is shown in Fig. 6: full transmission can be achieved.

3.3. Matrix with a TOF-E detector

Fig. 7 shows the matrix that we obtained with the TOF-E detector configuration for ${}^3\text{He}({}^4\text{He}, \gamma){}^7\text{Be}$ reaction. A ${}^4\text{He}^{2+}$ beam at $E_{{}^4\text{He}^{2+}} = 2.8 \text{ MeV}$ ($E_{cm} = 1.2 \text{ MeV}$) was used. It is possible to see the clear separation between

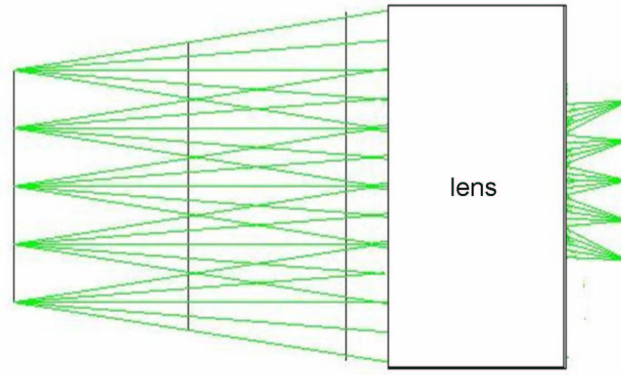


Fig. 6. From the left to the right respectively the carbon foil, electrostatic mirror, electrostatic mirror support, lens, MCP support and the MCP. We can see that the electrons (green line), with the introduction of the lens reach the MCP. The calculation is performed with COSY infinity.

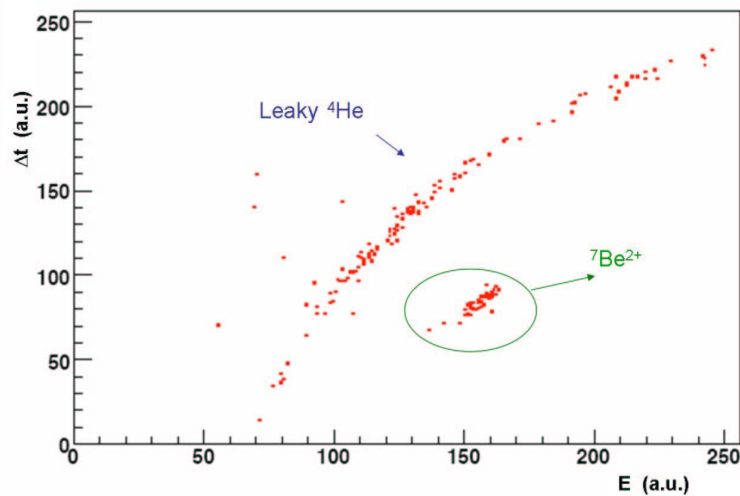


Fig. 7. Matrix with a TOF-E detector. On the y-axis is reported the time interval $\Delta t = t_d - \Delta t_{TOF}$, where t_d is the ~ 50 ns delay applied to the MCP signal (De Cesare 2006).

the leaky of the ${}^4\text{He}$ and the ${}^7\text{Be}^{2+}$ recoil nuclei.

cross-section at low energies, $E_{cm} = 0.7\text{-}1.1$ MeV.

The measured time resolution of 0.7 ns is good enough to separate the leaky from ${}^7\text{Be}$ recoils, Fig. 7.

4. Conclusions

The results show that a TOF-E detector is a suitable detector for measuring ${}^4\text{He}({}^3\text{He},\gamma){}^7\text{Be}$

The measurements are in progress and will be completed soon.

References

- Adelberger, E.G., et al. 1998, *RvMP*, 70, 1265
- Bemmerer, D., et al. 2006, *Phys. Rev. Lett.*, 97, 122502
- Busch, F., et al., 1980, *NIMPA*, 171, 71
- De Cesare, M. 2005-2006, Tesi di laurea, Università degli studi di Napoli Federico II
- Di Leva, A. 2002-2003, Tesi di laurea, Università degli studi di Napoli Federico II
- Gialanella, L., et al. 2004, *NIMPA*, 522, 432
- Haxton, W.C. 1995, *ARAA*, 33, 459
- Kuznetsov, A.V., et al. 2000, *NIMPA*, 452, 525
- Makino, K., & Berz, M. 2002, *NIMPA*, 427, 338
- Rogalla, D., et al., 1999, *NIMPA*, 437, 266
- Rogalla, D., et al. 2003, *NIMPA*, 513, 573
- Rolfs, C.E., & Rodney, W.S. 1988, *The University of Chicago Press*
- Schürmann, D., et al. 2004, *NIMPA*, 531, 428
- Serpico, P.D., et al. 2004, *MPP-82*
- Singh, B.S., et al. 2004, *Phys. Rev. Lett.*, 93, 262503
- Starzecki, W., et al. 1982, *NIMPA*, 193, 499
- Wiza, J.L. 1979, *Nucl. Instr. and Meth.*, 162, 587